

See discussions, stats, and author profiles for this publication at: <http://www.researchgate.net/publication/240789906>

# White mica domain formation: A model for paragonite, margarite, and muscovite formation during prograde metamorphism

ARTICLE *in* AMERICAN MINERALOGIST · APRIL 2008

Impact Factor: 1.96 · DOI: 10.2138/am.2008.2662

CITATIONS

8

READS

69

## 4 AUTHORS:



**Kenneth J. T. Livi**

Johns Hopkins University

78 PUBLICATIONS 1,301 CITATIONS

SEE PROFILE



**G.E. Christidis**

Technical University of Crete

48 PUBLICATIONS 690 CITATIONS

SEE PROFILE



**Péter Árkai**

Hungarian Academy of Sciences

47 PUBLICATIONS 561 CITATIONS

SEE PROFILE



**David R Veblen**

Johns Hopkins University

124 PUBLICATIONS 3,028 CITATIONS

SEE PROFILE

## White mica domain formation: A model for paragonite, margarite, and muscovite formation during prograde metamorphism

KENNETH J.T. LIVI,<sup>1,\*</sup> GEORGE E. CHRISTIDIS,<sup>2</sup> PÉTER ÁRKAI,<sup>3</sup> AND DAVID R. VEBLEN<sup>1</sup>

<sup>1</sup>The Morton K. Blaustein Department of Earth and Planetary Sciences, Johns Hopkins University, Baltimore, Maryland 21218, U.S.A.

<sup>2</sup>Technical University of Crete, Department of Mineral Resources Engineering, 73100, Chania, Greece

<sup>3</sup>Institute for Geochemical Research, Hungarian Academy of Sciences, Budaörsi út 45, 1112 Budapest, Hungary

### ABSTRACT

Scanning transmission electron microscopy images of the 00 $l$  white mica planes in crystals from central Switzerland and Crete, Greece, reveal that domains of paragonite, margarite, and muscovite are ordered within the basal plane. Energy dispersive X-ray analyses show that both cations in the interlayer and in the 2:1 layer have ordered on the scale of tens to hundreds of nanometers. Domain boundaries can be both sharp and crystallographically controlled or diffuse and irregular. A model outlining the domain formation process is presented that is consistent with X-ray powder diffraction and transmission electron microscopy data. The domain model incorporates aspects of a mixed-layered and a disordered compositionally intermediate phase models. The main feature of the model is the formation of mica species that segregate within the basal plane and contradict the notion of homogeneous layers within mixed-layer phases. Implications for the formation of all diagenetic and very low-grade metamorphic 2:1 sheet silicates are discussed.

**Keywords:** Muscovite, paragonite, margarite, TEM, STEM, low-grade metamorphism, white mica formation

### INTRODUCTION

Layered silicates—especially the 2:1 dioctahedral species—are the dominant reactants during diagenesis and very low-grade metamorphism (VLGM) of clastic sediments and igneous rocks. Be they smectite, saponite, mixed-layer phases, or illite at the lowest temperatures, or pyrophyllite, muscovite, paragonite, or margarite at higher temperatures, the cation occupancies of the 2:1 minerals reflect the relative metamorphic grade and the bulk composition of the system. Several reviews of the occurrences and crystal chemistry of micas have been written. Guidotti (1984) thoroughly reviewed the chemical variability of metamorphic micas above the greenschist facies. From this collection of data, it is obvious that micas adjust their chemical compositions to the physical conditions and bulk and fluid compositions during metamorphism. The basic context for interpretation of mica compositions is thermodynamic equilibrium.

Our understanding of low-temperature metamorphism is less complete than processes at higher grades. At subgreenschist conditions, the assumption of equilibrium is usually not valid; reactions are kinetically controlled, and most importantly, the reaction pathways become important. Therefore, an unambiguous understanding of a system requires a more complete description of the state of the minerals, including whether assemblages adhere to the phase rule, degree of compositional heterogeneity, surface energy issues such as size and grain boundary construction, and internal defect concentrations. To complicate matters, the fine-grained nature of low-grade minerals makes

this description more difficult.

From the earliest days of VLGM studies, X-ray powder diffraction (XRD) has been a powerful method for describing both short-range structural features, such as intercalation of different sheet structures, and average properties of many grains such as illite, and other sheet silicate crystallite sizes (Árkai 2002). Electron microprobe (EMP) and scanning electron microscope (SEM) analyses have been successfully used to determine chemical variations of low-grade minerals on the 2–5  $\mu\text{m}$  scale. However, many variations of composition and structure occur below this scale. Transmission electron microscopy (TEM) has made great advances in clarifying the non-periodic defect structures of phyllosilicates at low grades (Merriman and Peacor 1999).

The current investigation revisits the classic study of the very low- to low-grade metamorphic Liassic black clastic sediments of central Switzerland that began with Martin Frey (Frey 1969, 1978). From the Liassic shales, Frey described the evolution of the XRD patterns and mineral assemblages as metamorphism increased. This included the first description of a mixture of paragonite (Pg), muscovite (Ms), and an interstratified Pg/Ms (Frey 1969). This description was based on XRD intensities intermediate between Pg and Ms that were best observed in the (00,10) reflections. At the same time, Eugster et al. (1972) were describing the miscibility gap between Pg and Ms. It was therefore assumed that Na and K would not be found with significant solid solutions and must be separate phases. The interstratification was assumed to segregate Na and K onto separate planes and create separate and distinct Pg and Ms layers.

Combining these data with observations at lower and higher grades, Frey (1978) hypothesized that the kinetic steps toward

\* E-mail: klivi@jhu.edu

the formation of Pg were (1) formation of Na-rich smectite; (2) fixation of Na into interstratified Pg/Ms; and (3) recrystallization of Pg and Ms into discrete larger crystals. This model is called the mixed layer (ML) model here. In years to come, the number of occurrences of mixed Pg/Ms increased in pelites with sufficient aluminum and sodium. Livi et al. (1988) revisited samples from the Liassic shales exhibiting the interlayered Pg/Ms intermediate XRD intensities. They were not able to directly observe interstratified layers of Pg and Ms. However, there was indirect evidence that domains of Na- and K-rich regions existed within crystals that had intermediate Na-K bulk compositions.

Livi et al. (1997) expanded on their earlier work and outlined another reaction pathway. They proposed that the formation of Pg in the Liassic metaclastics starts with nanodomains of Na-rich mica-like structure, possibly brammallite (Na-illite), that coarsen and increase in Na content as metamorphism progresses. They proposed that the name “mixed Pg/Ms” be used unless the true state of the mixing is known. This model is called the domain model. Other important observations were that (1) the lowest grade smectite-rich samples contained little Na, and therefore, the process of domain formation cannot strictly be by exsolution, which requires a closed environment within a crystal. (2) Na-rich domains could exist below the resolution of the TEMs used at that time if viewed down  $\{hk0\}$  zones. Thus, analytical electron microscopy (AEM) analyses could be mixtures of domains and misleading. (3) Calculations of the structure factor for the superstructure reflection of an ordered 1:1 Pg:Ms intergrowth showed that these reflections would be very weak and would most likely be undetectable in XRD patterns. (4) XRD patterns for the ML and crystals with intermediate compositions would be very similar, differing only in the rationality of the reflections. Thus, it would be difficult to determine which of the two possibilities was correct.

We report here new scanning transmission electron microscopy (STEM) data from two localities that shed light on the growth mechanism of paragonite and margarite (Mrg) within muscovite. With these data we propose a revised mechanism for formation of white micas and comment on its implications for cation ordering in 2:1 sheet silicates in general.

## SAMPLES

STEM images were collected from two localities. One sample, MF-925, comes from the “type” locality of mixed layered Pg/Ms first described by Frey (1969). It is a white mica of epizonal grade from Gravera in the Central Swiss Alps. The Liassic Black Shales are an organic-rich shale with variable aluminum content. Phyllosilicates in the lowest grades (<100 °C) include illite, smectite, glauconite, chlorite, berthierine, and kaolinite. With increased low-grade metamorphism, smectite, berthierine and kaolinite are consumed and pyrophyllite and sudoite appear (250–300 °C). At and above the pyrophyllite isograd, Na-rich white micas also appear. At temperatures around 350–450 °C, margarite, and chloritoid form. At higher grades, biotite forms. Throughout the metamorphic sequence, EMP analyses of white micas tend to increase in total interlayer cation charge. TEM observations of mica textures show that crystal sizes increase and defect concentrations decrease (cf. Livi et al. 1997, 2002; Merriman and Frey 1999, p. 92–97, for further description).

The second sample comes from the Permian-Triassic Ravdoucha Beds in Crete, Greece, known as Tyros beds in south Peloponnese, at the base of the Trippolitza Unit, and is described in Christidis et al. (2003). The Ravdoucha beds comprise a volcano-sedimentary sequence characterized by anchizonal-epizonal pelites, sandstones, minor limestones, and intercalated volcanic rocks of intermediate-basic composition. The volcanic rocks have been affected by intensive hydrothermal alteration, which is associated with VMS Pb-Zn mineralization in South Peloponnese (Skarpelis 1982). Metamorphic conditions vary from ca. 2 kbar and 250–300 °C to 4–7 kbar and 350–400 °C representing different depths of burial for the various sectors of the Tyros strata (Baltatzis and Katagas 1984).

## EXPERIMENTAL METHODS

The STEM EDS and bright-field (BF) images were obtained by a Philips CM 300 FEG using the Emispec program ES Vision version 4 and an Oxford ultra-thin window light element detector. Grain mounts of white mica crystals were made by dry-grinding the samples and briefly dispersing them with ultrasound in a vial of tap water. This method was used to minimize the potential loss of Na or K to deionized water through cation exchange. Grids of holey-carbon support film on 100 and 200 mesh grids of both Be and Cu were dipped into the dilute suspension and dried. This produces samples with isolated crystals lying with  $c^*$  parallel to the beam direction. Note that this is a different orientation than the previous studies mentioned above. Crystal thicknesses were on the order of 100 nm as determined by electron energy-loss spectroscopy (Egerton 1996). Thus, each crystal was around 100 unit cells thick. In some maps, beryllium grids were used to minimize the interference of the Cu *L* with Na *K* X-ray peaks. Many crystals were analyzed in all samples, but many images were unusable due to loss of Na during analysis.

Several factors were important in the successful imaging of Na and K distributions: (1) the beam current needed to be sufficiently intense to obtain enough Na counts for good compositional contrast; (2) to minimize beam-induced Na loss, the probe was defocused after the initial dark field image was obtained. This reduces the flux of electrons while maintaining the current. (3) The images were first examined at low magnifications and fast scan rates to minimize sample-beam interactions. Scanning magnifications were between 40 and 70 kX. (4) Sample drift was reduced by allowing the sample and holder to thermally equilibrate with the microscope column for at least 2 h. Translation of the sample was kept to a minimum after equilibration. Under these conditions, the use of drift-correction software was not necessary. (5) The X-ray detector pulse processor rate was set at 4  $\mu$ s to maximize the throughput of X-ray pulses, but still maintain sufficient resolution to distinguish Cu *L* and Na *K* peaks. (6) A 1 s dwell time was used with pixel dimensions that varied around 60  $\times$  60. This resulted in a total acquisition time of more than an hour, with the actual time depending upon the dead time of the pulse processor. Some maps were taken over large areas and took as long as 5 h in overnight runs. And (7) the sample was tilted toward the detector by 10° and the detector crystal is inclined 20° toward the sample resulting in 30° takeoff angle.

In the ES Vision software, an entire EDS spectrum is collected in each pixel. This results in very large file sizes, but allows for the region-of-interest integration widths to be varied to obtain the best image contrast. This also allowed additional maps of Fe, S, Ca, and O, to be generated after the acquisition of the data cube. Spectra from areas of interest could be summed and quantitatively reduced to compositions. However, most summed spectra showed that there was a loss of interlayer cations during the acquisition. This did not effect the qualitative interpretation of Na and K segregation.

Because X-ray maps are not only a function of composition, but of sample thickness, the oxygen map proved to be a good proxy for thickness. This is because the concentration of O in micas would be relatively constant regardless of the Na and K content. Some images were normalized by the O intensity maps to minimize the effects of thickness.

## RESULTS

### STEM analysis

Results of STEM EDS analysis of sample MF-925 from Gravera, Switzerland are present in Figures 1 and 2. The Na,

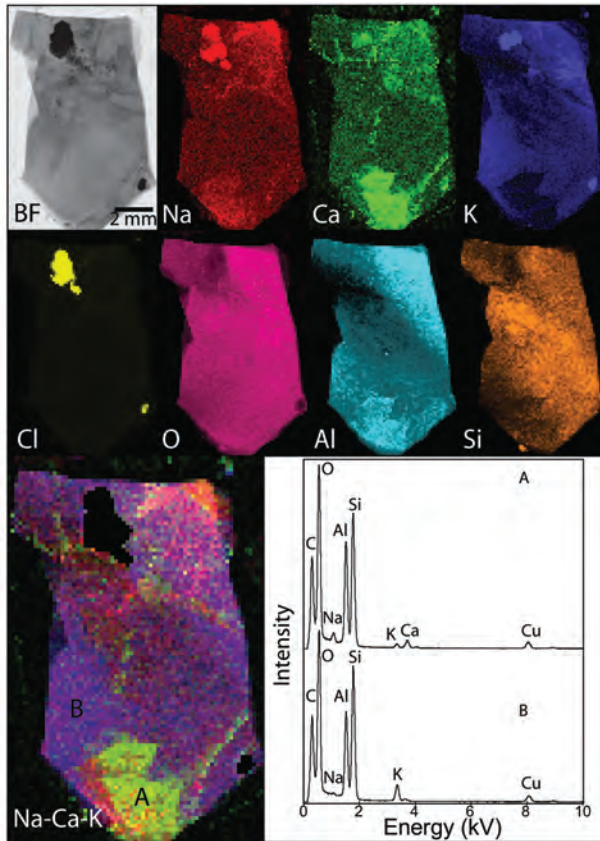


**FIGURE 1.** STEM EDS images of white mica flakes from Gravera, Switzerland (MF-925). The top half of the image includes a bright-field image (BF) and X-ray maps. The Na, Ca, and K images were combined to form a false-color RGB map (Na-Ca-K) of Pg (red), Mrg (green), and Ms (blue). The spectra summed from areas A and B are given in the lower right. The boundaries between Mrg and Ms (A and B) are sharp, indicating crystallographic control of lamellar orientation.

K, Ca, O, Si, Al, and Cl X-ray and the bright-field (BF) STEM images in Figure 1 came from a rather large crystal that had sharp crystal edges. There are several features worth mentioning in this sample. First, there are two areas that contain salts of KCl and NaCl. These are very bright in the Na, K, and Cl maps and dark in the O map and BF image. These represent daughter crystals of fluid inclusions within the mica crystal. Second, the O map is relatively uniform in intensity, but with some variation. Using O as a proxy for thickness, the upper right corner of the crystal is thicker than the lower and upper left. Third, K is anti-correlated with Na and Ca, while Na and Ca are well correlated. The region at the bottom of the crystal contains an area of high Ca and low K. This is a region of Mrg that is sharply defined in both the Ca and K maps—implying a crystallographic control of the boundary. Another line of high Ca is off to the right and is only faintly mimicked in the Na map because of low count rates for Na. Careful comparison of the Na and Ca maps in the lower part of the grain shows that a sliver of Pg is present close to the edge of the grain. Other regions of Pg can be seen in the upper right edge of the grain and by the lower intensity of K in the center of the crystal.

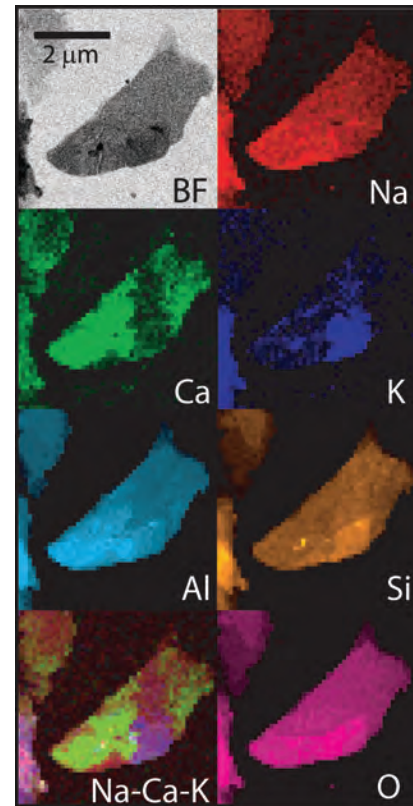


**FIGURE 2.** STEM EDS images of white mica from Gravera, Switzerland (MF-925). The interface between Pg and Ms are more irregular in this flake.

A false-color RGB composite was constructed using the intensities of Na (red), Ca, (green), and K (blue). Accordingly, Pg is red, Mrg is green, and Ms is blue. The salt crystals have been masked for clarity. From this image, it is clear that most of the crystal is muscovitic with three areas of paragonitic composition and one large area of Mrg with a few linear regions. Interestingly, the maps of Al and Si follow correlations expected for Mrg-Ms exchange components in that there is a decrease in Si and an increase in Al in the Mrg region.

Average spectra from areas labeled A and B on Figure 1 were generated by summing spectra for each pixel in the region of interest. Quantification of these spectra yields only half of the interlayer sites filled. Comparing these results to microprobe analyses of Livi et al. (1997) indicates that there was loss of alkali elements during acquisition. Therefore, although the relative abundance of Mrg, Pg, and Ms on a spatial scale can still be determined, the analyses cannot be considered quantitatively accurate. Figure 2 is another sample from Gravera that shows a complicated mixture of Pg, Mrg, and Ms. Margarite is the dominant phase in this crystal. The RGB composite was constructed in the same way as Figure 1. Most of the boundaries between the different phases are irregular, which is in contrast to Figure 1.

Figures 3 and 4 are images of samples from the Ravdoucha Beds, Crete. Figure 3 presents a striking image of intergrowths of Pg and Ms. No Ca was detected, and therefore, Mrg is absent. The O map indicates that a rounded flake lies over the largest

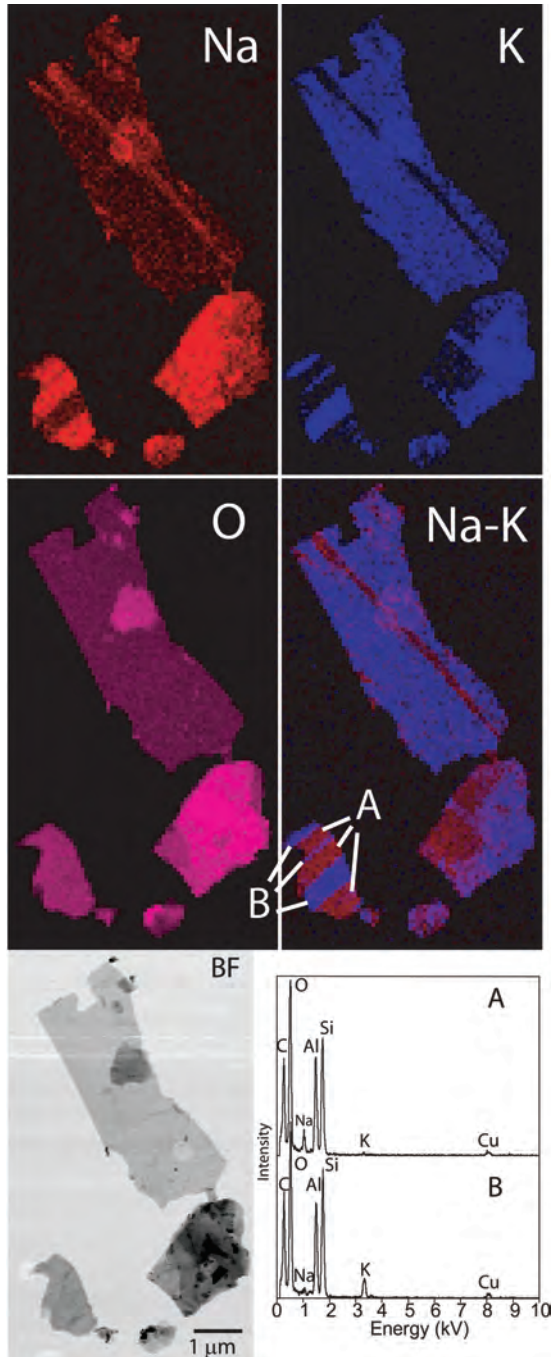


**FIGURE 3.** STEM EDS images of white mica flakes from the Ravdoucha beds, Crete (GR-5). This is the clearest and sharpest image of Pg and Ms segregation within the basal plane of the micas. Summed spectra from areas A and B show that not only are the interlayer cations well segregated, but that the Al/Si ratio also changes during segregation.

mica flake. Each of the individual crystals has different thicknesses and, therefore, produces different amounts of X-rays for a given composition. This effect was minimized by dividing the Na and K maps by the inverse of the O map and then combining them into the two-color image in the lower right. The lamellae of

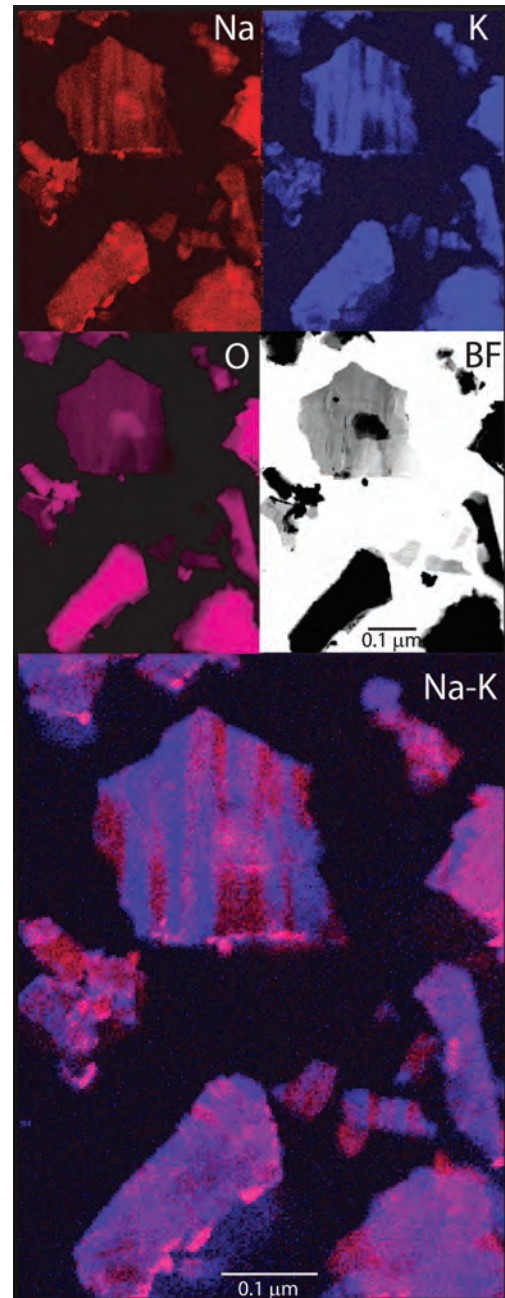


**FIGURE 4.** STEM EDS images of Cretan micas showing both more diffuse and sharp Pg/Ms boundaries.

Pg and Ms are sharp and indicate crystallographic control over boundary orientations. This is especially evident in the crystal in the lower left of the Na-K maps where the intergrowth creates zebra stripes. The summed spectra of all the Pg and Ms pixels in this small crystal are given at the bottom of Figure 3. Besides the obvious exchange of Na and K, there is a change in the Al/Si value with Pg (spectrum A) being more aluminous (minor Mg substitution in Ms can be seen in their spectra).

The sharpness of the lamellae does not vary with their orienta-

tion with respect to the EDS detector. This indicates that sample tilt and crystal orientation do not effect the apparent sharpness of lamellar boundaries. Therefore, these images reflect the true nature of the boundaries.

Figure 4 contains images from another sample from the Ravdoucha beds in Crete. The maps were thickness-normalized as in Figure 3. At the edges of some crystals, we can see an increase in Na and K. Spectra from these areas indicate that Na and K has likely leached from the micas and nucleated as  $K_2O$  and  $Na_2O$  at crystal edges. No Cl was detected. What is important in this figure is that the lamellae of Pg and Ms in the central large crystal are more irregular and have more diffuse boundaries than those in Figure 3. However, other neighboring crystals do contain the straight lamellae.

The STEM images for both samples show that within one crystal, there is a preferred direction of organization, but that some crystals contain lamellae with sharp boundaries while others are more diffuse. The diffuseness of the boundary could be explained by either a relict diffusion profile at the interface or that domains are overlapping each other in the  $c^*$  direction.

In the cases we describe in this paper, there is little unequivocal evidence for intermediate compositions contributing to the intensity between Pg and Ms. There were crystals showing compositions intermediate to Pg and Ms, but it was impossible to tell if this was due to overlap of domains or to a compositionally intermediate region. However, based on the images here, and the lattice-fringe images of Livi et al. (1997), the majority of mixed Pg/Ms crystals exhibit domain structures.

### XRD patterns

X-ray diffraction data for the Liassic sample is reproduced from Livi et al. (1997) and presented in Figure 5 along with new data from the Cretan sample. Both patterns show the distinct peaks for Pg and Ms and the intermediate intensity that been attributed to “mixed-layered” Pg/Ms. Frey (1969) identified this intermediate intensity as a 60:40 mix of Pg and Ms in samples from the same locality. In both samples, the location of the diffraction maximum for the mixed K/Na mica yields a  $00l$   $d$ -spacing of 9.75 Å instead of 9.80 Å for the 60:40 mix of Frey (Frey 1969). Note that Christidis et al. (2003) report  $d$ -spacings for the 001 diffraction maximum of this phase in the Ravdoucha beds varying between 9.70 and 9.85 Å. Finally in accordance with the STEM EDS data the Cretan sample does not contain Mrg layers.

## DISCUSSION

### Other examples of cation ordering within the interlayer

Veblen (1983) reported compositional domains cutting across the basal plane in the sheet silicate wonesite with a bulk composition of  $[(K,Na)_{0.5}\square_{0.5}][(Mg,Fe)_2Al_{0.5}](AlSi_3O_{10}(OH)_2$  (where  $\square$  represents a vacancy). The microstructure in wonesite was determined to be a mixture of exsolved talc and Na-biotite—the first reporting of exsolution in mica. The orientation of exsolution lamellae was thought to be due to the misfit of cell parameters leading to an optimal phase boundary (Bollman 1970; Robinson et al. 1971; Smelik and Veblen 1993) or kinetic factors. Veblen (1983) also hypothesized that segregation of interlayer cations

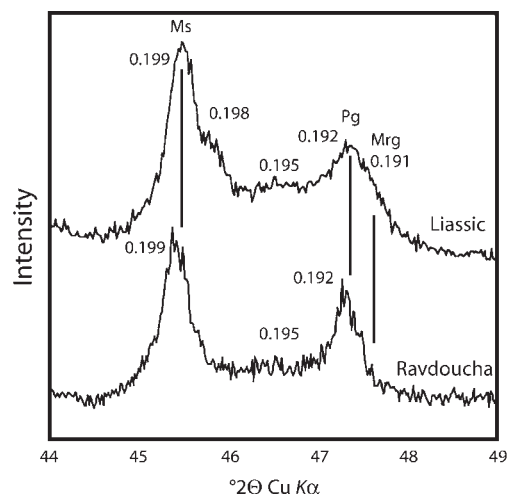


FIGURE 5. XRD patterns of the Liassic (from Livi et al. 1997) and Ravdoucha samples. Numbers above pattern are  $d$ -spacings in nanometers.

and vacancies within the basal plane occurred because this was the fast diffusion direction in micas.

Jiang and Peacor (1993) studied white micas formed during hydrothermal alteration of basalt from Wales and observed regions that had intermediate Na-K compositions. Selected area electron diffraction yielded patterns implying that those regions contained only a single phase. Thus, an alternative model was proposed—that an intermediate step to Pg formation was the formation of a homogeneous, yet compositionally intermediate, phase. Formation of Pg would then involve some exsolution and/or recrystallization at higher temperatures. This model is called the disordered compositionally intermediate model (DCI) here. Transmission electron microscopy evidence indicated that both the DCI phases and Pg form lamellae that occasionally cut across the basal plane of Ms. X-ray diffraction patterns also show an intermediate peak between Pg and Ms, but this peak was much sharper than profiles attributed to mixed-layered Pg/Ms. Similar results were obtained by Li et al. (1994) on mudrocks from the Central Wales. In addition, they describe images and diffraction patterns that suggest ordering of Na and K into separate layers and the formation of an 80 Å superstructure.

Giorgetti et al. (2003) also found evidence for DCI mica in hydrothermal retrograde alteration of eclogites. Based on XRD and TEM data, including EDS analyses, they argued that DCI regions were intergrown both parallel and oblique to coexisting Ms and Pg. An important conclusion they drew was that while both the DCI and mixed-layered models would produce intermediate XRD intensities, the DCI crystals would exhibit rational  $00l$  reflections while the mixed-layered crystals would be irrational. A statistical evaluation of the degree of irrationality of mixed layered vs. DCI phases has not been done, however.

Árkai et al. (2004) found intermediate intensities between Ms and Pg typically assigned to “mixed-layered” Pg/Ms. They demonstrated that small domains of Pg and Ms were segregated within the basal plane. They also found evidence for  $NH_4^+$  in the interlayer, although it was not determined if tobelite formed

domains or layers.

In a very different geologic setting, Mazzoli et al. (2001) reported on exsolution textures of paragonite in muscovite and proposed that they formed during a high-pressure phase of a complex polymetamorphic event. This is not analogous to the prograde processes described here. However, the “tweed” textures described therein corroborate the observation that Ms and Pg domains cut across crystal basal planes.

Meunier and Velde (2004) outlined possible ways in which substitutions of celadonite and pyrophyllite components may be theoretically distributed within illite. One of the possibilities was to cluster like cations within the octahedral layers, thus creating domains of celadonite or pyrophyllite. Infrared spectra of dioctahedral smectites led Besson and Drits (1997a, 1997b) and Zviagina et al. (2004) to conclude that there was an ordering of octahedral cations giving rise to pyrophyllite-like clusters within Mg- and Fe-bearing smectites. These “fragments” of pyrophyllite may be associated with interlayer cation ordering of vacancies, and thus be analogous to the present example. Vantelon et al. (2001, 2003) also found evidence from infrared and X-ray absorption spectroscopy for the ordering of octahedral cations in smectite. In a multiple analytical study of a Ni-Fe-Mg smectite, Decarreau et al. (1987) found evidence for the segregation of octahedral cations into trioctahedral and dioctahedral layers or domains. However, the data in these studies could not elucidate the distribution of the fragments, so it was not known whether the ordered clusters existed in domains cutting across or parallel to the basal plane or as homogeneous layers.

### Model for Pg, Mrg, and Ms formation

Livi et al. (1997) demonstrated that intermediate XRD intensities could be due to either mixed-layers or intermediate Na-K compositions. In addition, it was shown that the 001 reflection for an ordered 1:1 superstructure of Pg/Ms would have a very small structure factor, and therefore be difficult to detect. Livi et al. (1997) cautioned that the nature of the mixing of Pg and Ms could not be determined by XRD data alone.

An ordering of interlayer cations within the basal plane, especially Na and K, is in contrast to the conventional wisdom that layers within mixed-layer clay minerals are homogeneous; little thought is usually given to the compositional variation within the basal plane. This is not surprising since the size of the lamellae imaged here would not affect the shape or intensity of the  $hk0$  reflections in oriented X-ray powder diffraction (XRD) patterns, and thus would be largely undetectable by XRD.

The above textures require that a revised model for prograde formation of white mica species be developed that is consistent with the TEM and XRD data. We propose that the formation of discrete Pg, Ms, and Mrg follows a process of coarsening of nano-domains of immiscible interlayer cations during crystal growth. The steps may be outlined as follows: (1) At lowest grades, authigenic clay minerals may contain a wide range of cations inhomogeneously mixed within the interlayer. Kinetic barriers to ordering of cations into thermodynamically stable phases are high and two main groups exist—fixed layers (illite) and expandable layers (smectite) (Fig. 6a). The coexistence of illite and smectite may represent a state of metastable equilibrium or as a mixture of fundamental illite particles and interfaces. In Figure 6a, the

purple color denotes a disordered mixture of immiscible cations. The schematic XRD pattern to the right of Figure 6a depicts the peak for the fixed layer at 44–49 °2 $\theta$ . The exact position of the peak would depend on the average composition of the fixed layers. (2) With increased diagenesis/metamorphism, illite grows at the expense of smectite (Fig. 6b). The fixed layers will incorporate the three interlayer cations depending upon the bulk composition or upon the composition of an infiltrating fluid. It is not yet known if segregation of immiscible cations begins during diagenesis. (3) During high diagenesis/low anchizone Na + Ca segregates from K within the basal plane forming domains of Pg (and or Mrg) (B) and Ms (A) one layer thick in the 00 $l$  direction, but several unit cells wide in the  $hk0$  directions (Fig. 6c). This lowers the overall free energy of the system by lowering chemical potential gradients within the interlayer site. Disorder along the 00 $l$  direction creates the intermediate intensities in XRD patterns, while regions with sufficient coherent scattering sizes will produce distinct peaks. (4) Increased temperatures promote coarsening of domains within the 00 $l$  planes, and strain due to the mismatch of unit cells between layers builds. This strain energy is minimized by migration of the domains so that like layers lie next to each other (Fig. 6d). This will reduce the mixed-layered intensities while maximizing the discrete phase peaks. (5) Coarsening of domains continues until the interfaces between Pg, Mrg, and Ms are minimized (Figs. 6e and 6f) and discrete phases are produced.

In this model, intracrystalline bulk diffusion transport is needed in conjunction with crystal growth. One could make an argument against segregation on the basis that diffusion would be too slow at anchizone to epizone grades (200–450 °C) to promote domain formation. However, since it is unlikely that the intergrowths found in the Swiss and Cretan samples could have been formed by growth processes only, these textures are evidence that diffusion does indeed occur at low temperatures. What is unknown is how long it took for the textures to form.

The fast diffusion direction in micas is most likely within the interlayer—as opposed to across the tetrahedral-octahedral-tetrahedral (TOT) layer (Veblen 1983). Thus, it makes sense that immiscible cations would separate first within the basal plane before organizing across the TOT layers. Segregation of the Pg and Ms components could be a simple interdiffusion of Na<sup>+</sup> = K<sup>+</sup>. However, segregation of the Mrg component from Ms (or Pg) must involve a coupled substitution to maintain local charge balance. Two substitutions are most likely: (1) Ca<sup>2+</sup> + Al<sup>3+</sup> = K<sup>+</sup> + Si<sup>4+</sup>, or (2) Ca<sup>2+</sup> + □ = 2K<sup>+</sup>. Diffusion couple 1 requires the cooperative interdiffusion of four components in both the interlayer and 2:1 layer to maintain charge balance, while 2 involves only interlayer cations to maintain charge balance.

The analyses for coexisting domains in this study show that, by the time the domains coarsen to several tens of nanometers, not only have the interlayer cations segregated, but the tetrahedral and octahedral cations have also. The Pg domains have higher Al/Si than the Ms, which is found in more macroscopic coexisting white micas (Guidotti 1984). In the Mrg-rich Liassic samples, the composition of the 2:1 layer has become more Al-rich and Si-poor. This means that most of the original micas' structures have been exchanged. It is conceivable that in the early stages of segregation, the interlayer cations have diffused, but the 2:1 layer

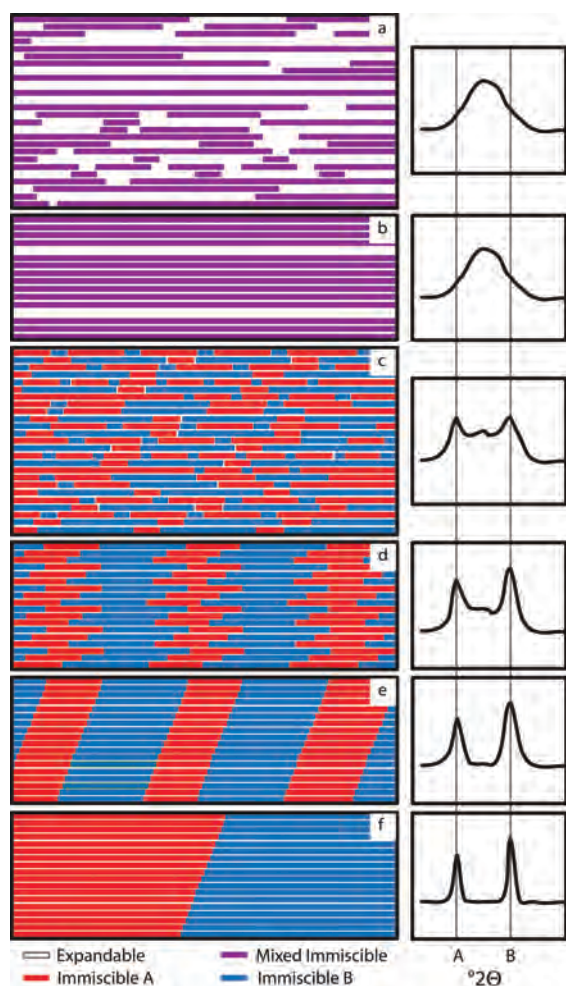


**FIGURE 6.** Diagram of the domain model. (a) Initial state of clay minerals dominated by fixed (purple) and expandable (white) layers, while the cations within the layers are thought to be disordered and contain immiscible cations in close proximity. Schematic XRD patterns are given on the right. (b) Growth of fixed layers at the expense of expandable. (c) Initiation of segregation of immiscible cations creates regions within the basal plane of relatively pure compositions. There is still disorder along the 00 $l$  direction. (d) Coarsening of domains creates strain energy due to mismatch of cell parameters across basal plane. This is minimized by alignment of like domains along 00 $l$ . (e, f) Minimization of grain boundaries (surface area reduction) leads to discrete grains.

cations have not yet adjusted since Al and Si coupled diffusion should lag behind Na and K. In this scenario, the segregation of Na and K lowers the chemical potential gradient,  $\Delta\mu$ , along the interlayer, but increases  $\Delta\mu$  across the 2:1 layer. In addition, strain energy increases as the size of the interlayer in adjacent domains become increasingly different. This increase in internal energy may be sufficient to overcome the activation energy for exchanging the 2:1 layer cations.

It would be tempting to describe this process as exsolution, but since it occurs during prograde metamorphism and crystal growth, matter from outside the crystal is added. Therefore, the process cannot be guaranteed to be a closed system, which is a requirement for exsolution. External sources of matter would

come from the metamorphic fluid, which would be active in the dissolution of metastable phases and small crystals within the rock. Regardless of the dominance of either diffusion or advection, the textures would be indistinguishable from those made by exsolution.

### Occurrences of “mixed” Pg/Ms

Frey (1987) summarized the minerals coexisting with “mixed” Pg/Ms in studies of metaclastites before 1987. More recent citations (or those not included in Frey 1987) are (1) associated with the Tethys; Austrian Alps (Kralik 1983), Meliata unit in the Western Carpathians (Árkai et al. 2003), Southern Carpathians (Ciulavu et al. 2001), Turkey (Yalçın and Bozkaya 1997; Bozkaya et al. 2002), Crete (Christidis et al. 2003; Árkai et al. 2001), Spain (Parras et al. 1996; Mata et al. 2001), Southwestern Portugal (Abad et al. 2001), and (2) non-Tethys localities; NW Argentina (Do Campo and Nieto 2003) and Trinidad (Frey et al. 1988). From these studies, the mineral assemblages associated with “mixed” Pg/Ms indicate that the most important parameter for the formation of “mixed” Pg/Ms is a relatively high aluminum content. The lowest grade occurrences of “mixed” Pg/Ms is high diagenetic to low anchizone (circa 200 °C). The two documented occurrences of the DCI micas differ from the majority of localities listed above by the fact that they are hydrothermal alterations of either plagioclase (Jiang and Peacor 1993) or higher grade eclogite phases (Giorgetti et al. 2003). Do Campo and Nieto (2003) presented TEM evidence for what might be the first description of DCI mica from a regional metamorphic pelite, but fell short of concluding that DCI micas were actually present.

### THE FUTURE

The three different models, mixed-layered, DCI, and domain, are not exclusive of each other. In fact, it is quite likely that products of all three processes can be found in the same rock or crystal. This makes the suggestion of Livi et al. (1997) to call samples exhibiting intermediate intensities as “mixed” Pg/Ms even more prudent. The model presented in this paper allows for the formation of all three types of “mixed” Pg/Ms textures. It may be that different metamorphic environments favor different parts of this process. Thus, regional metamorphism of clastic sediments where fluid fluxes are low may favor the mixed-layered and domain structures, whereas hydrothermal alteration may produce more DCI micas. More study is necessary to determine if this is valid.

It is quite likely that domain formation applies to other interlayer constituents. Thus, future investigations may show that toberlite (NH $_4^+$ ), vermiculite (Mg), and pyrophyllite (vacancies) formation also follow the domain model. If the process of domain formation is shown to be important during diagenetic conditions, it may be possible that smectite could be found as domains within illite. This is contrary to the concept of smectite being an interface between fundamental particles.

### ACKNOWLEDGMENTS

Electron microscopy was done at the Johns Hopkins University High-resolution Analytical Facility and was supported by a grant from the Keck Foundation and NSF grant EAR-0409071. We thank Margarita Do Campo and Warren Huff for helpful reviews. K.J.T.L. thanks John Ferry and Anne-Claire Galliot for many

discussions about mica and clay minerals. G.E.C. thanks the Greek Secretariat of Research and Development for funding under the auspices of the Greek-Hungarian bilateral collaboration programs. The work of P.Á. was supported by the Hungarian Research Fund (OTKA), Budapest, project no. T-049454/2005-2008.

## REFERENCES CITED

- Abad, I., Mata, M.P., Nieto, F., and Velilla, N. (2001) The phyllosilicates in diagenetic-metamorphic rocks of the South Portuguese zone, Southwestern Portugal. *Canadian Mineralogist*, 39, 1577–1589.
- Árkai, P. (2002) Phyllosilicates in very low-grade metamorphism: Transformation to micas. In A. Mottana, F.P. Sassi, J.B. Thompson, Jr., and S. Guggenheim, Eds., *Micas: Crystal Chemistry and Metamorphic Petrology*, 46, p. 463–478. *Reviews in Mineralogy and Geochemistry*, Mineralogical Society of America, Chantilly, Virginia.
- Árkai, P., Christidis, G., Manutsoglu, E., and Horváth, P. (2001) Preliminary results on the phyllosilicate reaction progress in the Permo-Triassic Ravdoucha (Tyros) beds of the External Hellenides (Crete, Greece). *Mid-European Clay Conference*, September 9–14, 2001, Stará Lesná, Slovakia, Book of Abstracts, p. 3.
- Árkai, P., Faryad, S.W., Vidal, O., and Balogh, K. (2003) Very low-grade metamorphism of sedimentary rocks of the Meliata unit, Western Carpathians, Slovakia: Implications of phyllosilicate characteristics. *International Journal of Earth Sciences*, 92, 68–85.
- Árkai, P., Livi, K.J.T., Frey, M., Brukner-Wein, A., and Sajgó, Cs. (2004) White micas with mixed interlayer occupancy: a possible cause of pitfalls in applying illite Kübler index “crystallinity” for the determination of metamorphic grade. *European Journal of Mineralogy*, 16, 469–482.
- Baltatzis, E.G. and Katagas, C.G. (1984) The pumpellyite-actinolite and contiguous facies in part of the Phyllite-Quartzite Series, Central North Peloponnese, Greece. *Journal of Metamorphic Geology*, 2, 349–363.
- Besson, G. and Drits, V.A. (1997a) Refined relationships between chemical composition of dioctahedral fine-grained mica minerals and their infrared spectra within the OH stretching region. Part I: Identification of the OH Stretching bands. *Clays and Clay Minerals*, 45, 158–169.
- (1997b) Refined relationships between chemical composition of dioctahedral fine-grained mica minerals and their infrared spectra within the OH stretching region. Part II: The main factors affecting OH vibrations and quantitative analysis. *Clays and Clay Minerals*, 45, 170–183.
- Bollman, W. (1970) *Crystal Defects and Crystalline Interfaces*. Springer-Verlag, New York.
- Bozkaya, Ö., Yalçın, H., and Göncüoğlu, M.C. (2002) Mineralogic and organic responses to stratigraphic irregularities: An example from the lower Paleozoic very low-grade metamorphic units of the Eastern Taurus Autochthon, Turkey. *Swiss Bulletin of Mineralogy and Petrology*, 82, 355–373.
- Christidis, G., Manutsoglu, E., and Árkai, P. (2003) K-, Na- and mixed Na-K-white micas in the Ravdoucha (Tyros) Beds and the Quartzite-Phyllite Formation, Crete: An indication for disequilibrium conditions of very low-temperature metamorphism. *EUROCLAY 2003—10<sup>th</sup> Conference of the European Clay Groups Association*, Modena, Italy, June 22–26, 2003, Abstracts, 66.
- Ciulavu, M., Ferreiro-Mahlmann, R., Seghedi, A., and Frey, M. (2001) Very low-grade metamorphism in the Danubian window, South Carpathians (Romania). *Terra Abstracts*, EUG 11, 230–231.
- Decarreau, A., Colin, F., Herbillon, A., Manceau, A., Nahon, D., and Paquet, H. (1987) Domain segregation in Ni-Fe-Mg-smectites. *Clays and Clay Minerals*, 35, 1–10.
- Do Campo, M. and Nieto, F. (2003) Transmission electron microscopy study of very low-grade metamorphic evolution in Neoproterozoic pelites of the Puncoviscana formation (Cordillera Oriental, NW Argentina). *Clay Minerals*, 38, 459–481.
- Egerton, R.F. (1996) *Electron Energy-Loss Spectroscopy in the Electron Microscope*, p. 485. Plenum Press, New York.
- Eugster, H.P., Albee, A.L., Bence, A.E., Thompson, J.B., and Waldbaum, D.R. (1972) The two phase region and excess mixing properties of paragonite ± muscovite crystalline solutions. *Journal of Petrology*, 13, 147–179.
- Frey, M. (1969) A mixed-layer paragonite/phengite of low-grade metamorphic origin. *Contributions to Mineralogy and Petrology*, 24, 63–65.
- (1978) Progressive low-grade metamorphism of a black shale formation, Central Swiss Alps, with special reference to pyrophyllite and margarite bearing assemblages. *Journal of Petrology*, 19, 95–135.
- (1987) *Low Temperature Metamorphism*, p. 351. Blackie, London.
- Frey, M., Saunders, J., and Schwander, H. (1988) The mineralogy and metamorphic geology of low-grade metasediments, Northern Range, Trinidad. *Journal Geological Society*, 145, 563–575.
- Giorgetti, G., Monecke, T., Kleberg, R., and Herzog, P.M. (2003) Intermediate sodium-potassium mica in hydrothermally altered rocks of the Waterloo deposit, Australia: a combined SEM-EMP-XRD-TEM study. *Contributions to Mineralogy and Petrology*, 146, 159–173.
- Guidotti, C.V. (1984) Micas in metamorphic rocks. In S.W. Bailey, Ed., *Micas*, 13, p. 357–467. *Reviews in Mineralogy*, Mineralogical Society of America, Chantilly, Virginia.
- Jiang, W.T. and Peacor, D.R. (1993) Formation and modification of metastable intermediate sodium potassium mica, paragonite, and muscovite in hydrothermally altered metabasalts from northern Wales. *American Mineralogist*, 78, 782–793.
- Kralik, M. (1983) Interpretation of K-Ar and Rb-Sr data from fractions of weakly metamorphosed shales and carbonate rock at the base of the Northern Calcareous Alps (Salzburg, Austria). *Mineralogy and Petrology*, 32, 49–67.
- Li, G., Peacor, D.R., Merriman, R.J., and Roberts, B. (1994) The diagenetic to low-grade metamorphic evolution of matrix white micas in the system muscovite-paragonite in a mudrock from central Wales, United Kingdom. *Clays and Clay Minerals*, 42, 369–381.
- Livi, K.J.T., Veblen, D.R., and Ferry, J.M. (1988) Electron microscope study of anchizone and epizone metamorphosed shales from the central Swiss Alps (abstract). *Geological Society of America, Abstracts and Program*, 20, A244.
- Livi, K.J.T., Veblen, D.R., Ferry, J.M., and Frey, M. (1997) Evolution of 2:1 layered silicates in low-grade metamorphosed Liassic shales of central Switzerland. *Journal of Metamorphic Geology*, 15, 323–344.
- Livi, K.J.T., Veblen, D.R., Ferry, J.M., Frey, M., and Connolly, J.A.D. (2002) Reactions and physical conditions during metamorphism of Liassic aluminous black shales and marls in central Switzerland. *European Journal of Mineralogy*, 14, 647–672.
- Mata, M.P., Nieto, F., and López-Aguayo, F. (2001) Estudio por SEM y TEM de interestratificados cookeita-paragonita en metapelitas de bajo grado de la Cuenca de Cameros (Soria-La Rioja). *Geotemas*, 1, 43–46.
- Mazzoli, C., Sassi, R., and Baronnet, A. (2001) A peculiar Ms-Pg textural association in a chloritoid-bearing micaschist recording a multistage *P-T* path. *European Journal of Mineralogy*, 13, 1127–1138.
- Merriman, R.J. and Frey, M. (1999) Patterns of very low-grade metamorphism in metapelitic rocks. In M. Frey and D. Robinson, Eds., *Low-grade metamorphism*, p. 61–107. Blackwell Science Ltd., Oxford.
- Merriman, R.J. and Peacor, D.R. (1999) Very low-grade metapelites: Mineralogy, microfabrics and measuring reaction progress. In M. Frey and D. Robinson, Eds., *Low-grade Metamorphism*, p. 10–60. Blackwell Science Ltd., Oxford.
- Meunier, A. and Velde, B. (2004) Illite, p. 286. Springer, Berlin.
- Parras, J., Sánchez-Jiménez, C., Rodas, M., and Luque, F.J. (1996) Ceramic applications of Middle Ordovician shales from central Spain. *Applied Clay Science*, 11, 25–41.
- Robinson, P., Jaffe, H.W., Ross, M., and Klein, C. (1971) Orientation of exsolution lamellae in clinopyroxenes and clin amphiboles: Consideration of optimal phase boundaries. *American Mineralogist*, 56, 909–939.
- Skarpelis, N.S. (1982) Metallogeny of massive sulfides and petrology of the external metamorphic belts of the Hellenides (SE Peloponnese). Ph.D. thesis, University of Athens, Greece.
- Smelik, E.A. and Veblen, D.R. (1993) A transmission and analytical electron microscope study of exsolution microstructures and mechanisms in the ortho-amphiboles anophyllite and gedrite. *American Mineralogist*, 78, 511–532.
- Vantelon, D., Pelletier, M., Michot, L.J., Barres, O., and Thomas, F. (2001) Fe, Mg and Al distribution in the octahedral sheet of montmorillonites. An infrared study in the OH-bending region. *Clay Minerals*, 36, 369–379.
- Vantelon, D., Montarges-Pelletier, E., Michot, L.J., Brioso, V., Pelletier, M., and Thomas, F. (2003) Iron distribution in the octahedral sheet of dioctahedral smectites. An Fe K-edge X-ray absorption spectroscopy study. *Physics and Chemistry of Minerals*, 30, 44–53.
- Veblen, D.R. (1983) Exsolution and crystal chemistry of the sodium mica wonesite. *American Mineralogist*, 68, 498–504.
- Yalçın, H. and Bozkaya, Ö. (1997) Kangal-Alacahan yöresi (Sivas) Üst Paleozoyik yaşlı meta-sedimanter kayalarda gömülme ve bindirme ile ilişkili çok düşük dereceli metamorfizma. *Geological Bulletin of Turkey*, 40, 1–16.
- Zviagina, B.B., McCarty, D.K., Srodon, J., and Drits, V.A. (2004) Interpretation of infrared spectra of dioctahedral smectites in the region of OH-stretching vibrations. *Clays and Clay Minerals*, 52, 399–410.

MANUSCRIPT RECEIVED APRIL 3, 2007

MANUSCRIPT ACCEPTED NOVEMBER 16, 2007

MANUSCRIPT HANDLED BY WARREN HUFF